Multichannel quantum defect theory for ro-vibrational transitions in ultracold molecule-molecule collisions

Jisha Hazra

Department of Chemistry, University of Nevada Las Vegas, Las Vegas, Nevada 89154

Brandon P. Ruzic

JILA, NIST, and Department of Physics,

University of Colorado, Boulder, Colorado 80309, USA

N. Balakrishnan

Department of Chemistry, University of Nevada Las Vegas, Las Vegas, Nevada 89154

John L. Bohn

JILA, NIST, and Department of Physics,

University of Colorado, Boulder, Colorado 80309, USA

(Dated: August 6, 2014)

arXiv:1408.0834v1 [physics.atom-ph] 4 Aug 2014

Abstract

Multichannel quantum defect theory (MQDT) has been widely applied to resonant and non-resonant scattering in a variety of atomic collision processes. In recent years, the method has been applied to cold collisions with considerable success, and it has proven to be a computationally viable alternative to full-close coupling (CC) calculations when spin, hyperfine and external field effects are included. In this paper, we describe a hybrid approach for molecule-molecule scattering that includes the simplicity of MQDT while treating the short-range interaction explicitly using CC calculations. This hybrid approach, demonstrated for H_2-H_2 collisions in full-dimensionality, is shown to adequately reproduce cross sections for quasi-resonant rotational and vibrational transitions in the ultracold (1μK) and $\sim$ 1-10 K regime spanning seven orders of magnitude. It is further shown that an energy-independent short-range K-matrix evaluated in the ultracold regime (1μK) can adequately characterize cross sections in the mK-K regime when no shape resonances are present. The hybrid CC-MQDT formalism provides an alternative approach to full CC calculations at considerably less computational expense for cold and ultracold molecular scattering.

PACS numbers: 34.50.-s, 67.85.-d

I. INTRODUCTION

Molecules in a translationally cold gas present a particular perspective on collisions and chemistry. One the one hand, atoms in the colliding molecules exchange energy on the scale of tens to thousands of Kelvin, driven by deep potential energy surfaces. On such surfaces occur rotational, vibrational, and chemical transformations. On the other hand, the ability of the molecules to initiate this activity is strongly dependent on behavior at the μK - mK translational energy scales of the gas. The slowly moving molecules, to get close enough to react, must first negotiate their way through the long-range forces acting between them. These forces, negligible at room temperature, loom large in the ultracold. The dominance of long-rage forces had led to *control* over chemical reaction, by, for example, the simple expedient of applying a modest electric field to alter the dipole moments of molecules [1]. For this reason cold molecules are seen as novel tools for probing and controlling chemistry with unprecedented resolution [2].

This dichotomy of energy scales presents a unique point of view for theories of molecules interacting at ultracold temperatures, which must now account for dynamics occurring over many orders of magnitude in energy. Luckily, the energy dichotomy relates in a direct way to motion on disparate spatial scales. Specifically, the full, energy-sharing dynamics of atoms in the collision complex occurs where all participating atoms are close together, whereas the long-range dynamics occurs between well-delineated collision partners that are far apart. The business of cold collision theory is to accurately account for the relatively straightforward long-range dynamics, while incorporating, to the extent desirable or reasonable, the short-range dynamics.

The separation into short- and long-range physics finds its natural expression in the multichannel quantum defect theory (MQDT), whose origins go back to understanding spectra of Rydberg atoms [3–5], but which has been successfully extended to more general contexts [6, 7], including cold collisions of atoms [8–12], atoms and ions [13, 14], atoms and molecules [15, 16], and molecule-molecule reactive scattering [17–20]. In all cases, long-range wave functions are carefully constructed and then matched to a wave function that is a suitable representation of the short-range physics. Depending on the context, the short-range physics can be successfully treated in a schematic way by (for example) positing absorbing boundary conditions to represent chemical reactions [17, 18, 20] or, in the case of alkali atom cold

collisions, by means of simple spin-dependent phase shifts [8, 21].

In this article we tackle head-on the complete short-range dynamics of molecule-molecule scattering for the comparatively straightforward case of H_2+H_2 collisions at collision energies $\leq$ 10 K, where comparison with numerically accurate scattering calculations can be made. A main finding is that the MQDT approach can be accurate and considerably more efficient numerically, provided sufficient care is taken in constructing the long-range wave functions. Thus short-range and long-range dynamics can be successfully welded together in this important prototype case where energy can be exchanged between rotational and vibrational degrees of freedom of two molecules. The calculations presented here represent a first, necessary step toward adapting MQDT methods to the broader problem of cold chemistry, which should ultimately lead to understanding how to manipulate reaction dynamics in realistic ultracold gases.

The paper is organized as follows. In section II we present in detail the close-coupling (CC) and MQDT formalisms for non-reactive scattering in collisions between two $^1\Sigma$ molecules. In section III we provide numerical illustration of the method for quasi-resonant rotational and vibrational transitions in H_2-H_2 collisions, including both ortho and para symmetries. Conclusions and future directions are presented in section IV.

II. THEORY

A. Quantum close-coupling approach for molecule-molecule collisions

The molecule-molecule scattering theory for collisions of two $^1\Sigma$ diatomic molecules has been well established and described in detail in many prior works [23–27]. Only a brief description to introduce the key terminologies and set the stage for the MQDT formalism is given here. The full close coupling (CC) [28] methodology based on the solution of the time-independent Schrödinger equation is used to solve the four-body scattering problem in Jacobi coordinates. After elimination of center-of-mass motion, the Hamiltonian for the relative motion of two H_2 molecules in space-fixed coordinates may be written as

$$\hat{H} = -\frac{\hbar^2}{2\mu}\frac{\partial^2}{\partial R^2} + \frac{\hat{\ell}^2}{2\mu R^2} + \sum_{i=1}^{2} \hat{h}_i(r_i) + U(\mathbf{r_1}, \mathbf{r_2}, \mathbf{R}) \tag{1}$$

where $\mathbf{R}$ is the vector joining the center of mass of the two H_2 molecules, μ and $\hat{\ell}$ are the reduced mass and orbital angular momentum of the two colliding H_2 molecules and $U(\mathbf{r_1}, \mathbf{r_2}, \mathbf{R})$ is the interaction potential. The terms, $\hat{h}_i(r_i),\ i = 1, 2$ are the Hamiltonians of the two isolated H_2 molecules:

$$\hat{h}_i(r_i) = -\frac{\hbar^2}{2\mu_i}\frac{\partial^2}{\partial r_i^2} + \frac{\hat{j}_i^2}{2\mu_i r_i^2} + V(r_i) \tag{2}$$

where r_i, μ_i, and $\hat{j}_i$ are the internuclear separation, reduced mass, and the rotational angular momenta of the two separated H_2 molecules. The H_2-H_2 interaction potential is expanded in terms of coupled spherical harmonics [24]

$$U(\mathbf{r_1}, \mathbf{r_2}, \mathbf{R}) = \sum_{\lambda} A_\lambda(r_1, r_2, R) Y_\lambda(\hat{r_1}, \hat{r_2}, \hat{R}) \tag{3}$$

with

$$Y_\lambda(\hat{r_1}, \hat{r_2}, \hat{R}) = \sum_{m_\lambda} \langle \lambda_1 m_{\lambda_1} \lambda_2 m_{\lambda_2} | \lambda_{12} m_{\lambda_{12}} \rangle \times Y_{\lambda_1 m_{\lambda_1}}(\hat{r_1}) Y_{\lambda_2 m_{\lambda_2}}(\hat{r_2}) Y^*_{\lambda_{12} m_{\lambda_{12}}}(\hat{R}) \tag{4}$$

where $\lambda \equiv \{\lambda_1, \lambda_2, \lambda_{12}\}$ and $m_\lambda \equiv \{m_{\lambda_1}, m_{\lambda_2}, m_{\lambda_{12}}\}$. The indices λ_1, λ_2 and λ_{12} are non-negative integers and the sum of these three quantities must be an even integer. The homonuclear symmetry of H_2 requires that λ_1 and λ_2 must be even. The quantity in angular brackets of the above equation is a Clebsch-Gordan coefficient, and $Y_{\lambda m_\lambda}$ are spherical harmonics. The Schr̈odinger equation is conveniently formulated by introducing the total angular momentum representation [28]. The total angular momentum $\overrightarrow{J} = \overrightarrow{j_{12}} + \overrightarrow{\ell}$ is the vector sum of total rotational angular momentum $\overrightarrow{j_{12}} = \overrightarrow{j_1} + \overrightarrow{j_2}$ of the two molecules and orbital angular momentum $\overrightarrow{\ell}$. Note that all molecules remain in singlet electronic spin states, so we suppress this notation in the following. For collisions between two indistinguishable molecules, the total wave function Ψ may be expanded in terms of rotational and vibrational wave functions of the two H_2 molecules, $\Phi_{vj\ell}^{JM\epsilon_I\epsilon_P}$, in the total angular momentum representation [28]:

$$\Psi(\mathbf{r_1}, \mathbf{r_2}, \mathbf{R}) = \frac{1}{R} \sum_{v,j,\ell,J,M} F_{vj\ell}^{JM\epsilon_I\epsilon_P}(R) \Phi_{vj\ell}^{JM\epsilon_I\epsilon_P}(\mathbf{r_1}, \mathbf{r_2}, \mathbf{R}) \tag{5}$$

where $F_{vj\ell}^{JM\epsilon_I\epsilon_P}(R)$ are the radial expansion coefficients, $v \equiv v_1, v_2$ represents the vibrational quantum numbers and $j \equiv j_1, j_2$ specifies the rotational quantum numbers of the two diatomic fragments. The quantity $\epsilon_I = (-1)^{j_1+j_2+\ell}$ is the eigenvalue of the spatial inversion

operator, and ϵ_P is the eigenvalue of the exchange permutation symmetry operator for two H_2 molecules (for the indistinguishable case, e.g., para-para or ortho-ortho). The explicit expression for $\Phi_{vj\ell}^{JM\epsilon_I\epsilon_P}$ is given in Eqs. (6), (8) and (15) of Ref. [27]. The radial expansion coefficients $F_{vj\ell}^{JM\epsilon_I\epsilon_P}$ are evaluated by solving the close-coupled radial equations in R,

$$\left(-\frac{\hbar^2}{2\mu}\frac{d^2}{dR^2}+\frac{\hbar^2\ell(\ell+1)}{2\mu R^2}+\epsilon_{vj}-E\right)F_{vj\ell}^{JM\epsilon_I\epsilon_P}(R) + \sum_{v',j',\ell'}\mathcal{U}_{vj\ell,v'j'\ell'}^{JM\epsilon_I\epsilon_P}(R)F_{v'j'\ell'}^{JM\epsilon_I\epsilon_P}(R)=0 \tag{6}$$

resulting from substitution of Eqs. (1) and (5) in the time-independent Schrödinger equation $H\Psi = E\Psi$. Here E is the total energy of the system, and we define the collision energy to be $E_c = E - \epsilon_{v_1j_1} + \epsilon_{v_2j_2} = E - \epsilon_{vj}$. The symbol $\epsilon_{v_ij_i}(i=1,2)$ denotes the asymptotic ro-vibrational energies of the two H_2 molecules. Under molecule permutation the interaction potential, $\mathcal{U}_{vj\ell,v'j'\ell'}^{JM\epsilon_I\epsilon_P}(R)$, is given by

$$\mathcal{U}_{vj\ell,v'j'\ell'}^{JM\epsilon_I\epsilon_P}(R)=\Delta_{vj_1j_2}\Delta_{v'j_1'j_2'}[\mathcal{U}_{vj\ell,v'j'\ell'}^{JM\epsilon_I}(R)+\epsilon_P(-1)^{j_1'+j_2'+j_{12}'+\ell'}\mathcal{U}_{vj\ell,\bar{v}'\bar{j}'\ell'}^{JM\epsilon_I}(R)], \tag{7}$$

where $\bar{v}=v_2v_1$ and $\bar{j}=j_2j_1j_{12}$, $\epsilon_P=\pm1$, and $\Delta_{vj_1j_2}=[2(1+\delta_{v_1v_2}\delta_{j_1j_2})]^{-1/2}$. The matrix elements of the interaction potential, $\mathcal{U}_{vj\ell,v'j'\ell'}^{JM\epsilon_I}(R)$, are defined as

$$\mathcal{U}_{vj\ell,v'j'\ell'}^{JM\epsilon_I}(R)=\sum_{\lambda}B_{vj_1j_2,v'j_1'j_2'}^{\lambda\epsilon_I}(R)f_{jl,j'l'}^{J;\lambda} \tag{8}$$

where the radial elements $B_{vj_1j_2,v'j_1'j_2'}^{\lambda\epsilon_I}(R)$ are given by

$$B_{vj_1j_2,v'j_1'j_2'}^{\lambda\epsilon_I}(R)=\int_0^\infty\int_0^\infty\chi_{vj_1j_2}^{\epsilon_I}(r_1,r_2)A_\lambda^{\epsilon_I}(r_1,r_2,R)\chi_{v'j_1'j_2'}^{\epsilon_I}(r_1,r_2)dr_1dr_2, \tag{9}$$

and the function $f_{jl,j'l'}^{J;\lambda}$ is given in terms of $3-j$, $6-j$, and $9-j$ symbols:

$$f_{jl,jl}^{J;\lambda}=(4\pi)^{-3/2}(-1)^{j_1+j_2+j_{12}'+J}[\lambda,j,l,j',l',\lambda_{12}]^{1/2} \begin{pmatrix} j_1 & j_1' & \lambda_1\\ 0 & 0 & 0\end{pmatrix}\begin{pmatrix} j_2 & j_2' & \lambda_2\\ 0 & 0 & 0\end{pmatrix}\begin{pmatrix} l & l' & \lambda_{12}\\ 0 & 0 & 0\end{pmatrix} \begin{Bmatrix} l & l' & \lambda_{12}\\ j_{12}' & j_{12} & J\end{Bmatrix}\begin{Bmatrix} j_{12}' & j_2' & j_1'\\ j_{12} & j_2 & j_1\\ \lambda_{12} & \lambda_2 & \lambda_1\end{Bmatrix}, \tag{10}$$

with the notation

$$[x_1,x_2,...,x_n]=(2x_1+1)(2x_2+1)...(2x_n+1). \tag{11}$$

In the coupled-channel formalism, either the wave function $\mathbf{F}(R)$ and its derivative $\mathbf{F'}(R)$ or the log-derivative matrix $\mathbf{Y} = \mathbf{F'F^{-1}}$ is propagated from a point in the classically forbidden region near the origin, $R \sim 0$, to where the interaction potential becomes negligible, R_∞. In the present case, the CC equation for each value of R is solved by propagating the log-derivative matrix $\mathbf{Y}$ by following the methods of Johnson and Manolopoulos [29, 30]. The scattering matrix $\mathbf{S}$ for specific values of J, ϵ_I and ϵ_P is evaluated by matching the $\mathbf{Y}$ matrix to known asymptotic solutions of the CC equations at R_∞. The boundary condition is

$$(\mathbf{YJ} - \mathbf{J'}) = (\mathbf{YN} - \mathbf{N'})\mathbf{K}. \tag{12}$$

The matrices $\mathbf{J}$ (not to be confused with the total angular momentum) and $\mathbf{N}$ are diagonal matrices of asymptotic functions. For convenience, the total number of coupled-channels N is partitioned into N_o open channels (with $E > 0$) and N_c closed channels (with $E \leq 0$) such that $N = N_o + N_c$. For the open channels N_o these functions are known as Riccati-Bessel functions, and for the closed channels N_c they are modified spherical Bessel functions of the first and third kinds [31]. $\mathbf{J'}$ and $\mathbf{N'}$ are the derivative matrices of $\mathbf{J}$ and $\mathbf{N}$, respectively. For an N channel problem the scattering $\mathbf{S}$ matrix is easily calculated by considering only the open-open sub-block of $\mathbf{K}$ matrix by the following expression

$$\mathbf{S} = (1 + i\mathbf{K}_{oo})^{-1}(1 - i\mathbf{K}_{oo}). \tag{13}$$

Finally, the state-to-state cross section is obtained from the $\mathbf{S}$ matrix. For indistinguishable molecule collisions one must symmetrize the cross-section with the statistically weighted sum of the exchange-permutation symmetry components. Explicit expressions for state-to-state cross section with and without exchange symmetry have been given in prior publications [27, 32]. For completeness, and for the ease of comparisons with MQDT results, the expressions for the symmetrized cross sections are reproduced below:

$$\sigma_{v_1 j_1 v_2 j_2 \to v_1' j_1' v_2' j_2'}(E_c) = W^+ \sigma^{\epsilon_P = +1} + W^- \sigma^{\epsilon_P = -1} \tag{14}$$

with

$$\sigma^{\epsilon_P} = \frac{\pi(1 + \delta_{v_1 v_2}\delta_{j_1 j_2})(1 + \delta_{v_1' v_2'}\delta_{j_1' j_2'})}{(2j_1 + 1)(2j_2 + 1)k^2} \tag{15}$$

$$\times \sum_{j_{12} j_{12}' \ell \ell' J \epsilon_I} (2J + 1)|\delta_{vj\ell, v'j'\ell'} - S^{J\epsilon_I \epsilon_P}_{vj\ell, v'j'\ell'}(E_C)|^2 \tag{16}$$

where $k^2 = 2\mu E_c/\hbar^2$. In the case of collisions of two ortho-H_2 molecules having nuclear spin $I = 1$ and weight factors $W^+ = 2/3$ and $W^- = 1/3$, one must consider both exchange permutation symmetries $\epsilon_P = \pm 1$ for the calculation of state-to-state cross sections. For collisions between two para-H_2 molecules with nuclear spin $I = 0$ and weight factors $W^+ = 1$ and $W^- = 0$, only one exchange-permutation symmetry $\epsilon_P = +1$ is required for evaluating the cross-section. To describe the state-to-state cross-section between two H_2 molecules, we use the term "combined molecular state", CMS, which denotes the combined ro-vibrational quantum numbers of the two molecules. In this notation, the collision of the first H_2 molecule having the ro-vibrational state (v_1, j_1) with the second H_2 molecule in state (v_2, j_2) is denoted by a unique term (v_1, j_1, v_2, j_2). This CMS is the quantum state which characterizes the molecule-molecule system before or after the collision.

It should be emphasized that the CC method described here is a numerically exact calculation that incorporates the complete four-body physics of the collision complex, provided that sufficiently many channels are included in the calculation (which is certainly possible for light molecules such as H_2). This method does, however, require the complete calculation to be performed separately for each collision energy of interest. The number of such calculations may be large, say in the case where cross sections vary with energy due to resonances or (at ultracold temperature) due to the Wigner threshold laws. Restricting this requirement of calculations at many energies is a main accomplishment of the MQDT method, to which we now turn.

B. The MQDT Formalism

The MQDT formalism modifies the scattering calculations in several ways. First, it acknowledges that, beyond a certain interparticle spacing R_m, the scattering channels become independent from one another, and their wave functions can be constructed in each channel individually. This leads to a reduction in computational time since the number of arithmetic operations is proportional to N^3 for the CC calculation. Whereas, this number is only proportional to N for the MQDT calculation. Second, it notes that this distance R_m can often be chosen small enough that all channels are "locally open," meaning that the kinetic energy at R_m is positive in each channel. In this circumstance, boundary conditions in closed channels need not yet be applied, and the wave function at R_m will not have the

sensitive energy dependence required near resonances.

Third, the asymptotic wave functions to which one matches the short-range wave function are themselves chosen to exhibit weak energy dependence, so that the resulting short-range K-matrix, $\mathbf{K}^{\rm sr}$, is only weakly dependent on energy and magnetic field. This allows for efficient calculations over a wide range of energy and field. Features such as resonances and Wigner threshold laws are then recovered at a later stage via relatively simple algebraic procedures. This method has proven useful and economical in molecular scattering [6] and in ultracold collisions [8]. Here we describe its application to the H_2-H_2 cold collision problem.

$\mathbf{K}^{\rm sr}$ is defined by writing the matrix wavefunction, $\mathbf{M}$, in terms of MQDT reference functions, $\hat{f}$ and $\hat{g}$,

$$M_{ij} = \hat{f}_i \delta_{ij} - \hat{g}_i K_{ij}^{sr} \quad \text{for } R \geq R_m \tag{17}$$

where $\mathbf{M}$ is a $N \times N$ matrix that contains N wavefunctions with physical boundary conditions at the origin. $\mathbf{K}^{\rm sr}$ is obtained by matching the log-derivative of $\mathbf{M}$ to the log-derivative matrix $\mathbf{Y}$ at R_m

$$\mathbf{M}'\mathbf{M}^{-1} = \mathbf{Y} \tag{18}$$

$$\mathbf{K}^{\rm sr} = (\mathbf{Y}\hat{g} - \hat{g}')^{-1}(\mathbf{Y}\hat{f} - \hat{f}'). \tag{19}$$

To achieve a weakly energy and field dependent $\mathbf{K}^{\rm sr}$, we let $\hat{f}$ and $\hat{g}$ have WKB-like boundary conditions well within the classically allowed region at $R = R_x \leq R_m$ [6, 33],

$$\hat{f}_i(R) = \frac{1}{\sqrt{k_i(R)}} \sin\left(\int_{R_x}^{R} k_i(R')dR' + \phi_i\right) \text{ at } R = R_x \tag{20}$$

$$\hat{g}_i(R) = -\frac{1}{\sqrt{k_i(R)}} \cos\left(\int_{R_x}^{R} k_i(R')dR' + \phi_i\right) \text{ at } R = R_x \tag{21}$$

where ϕ_i denotes an energy independent phase described by Ruzic et al. [22]. Here, $k_i(R) = \sqrt{\frac{2\mu}{\hbar^2}\left(E - \epsilon_{v_i j_i} - V_{ii}(R)\right)}$, and the derivatives of $\hat{f}$ and $\hat{g}$ at R_x are defined by the full, radial derivatives of equations (20) and (21).

One obtains $\hat{f}$ and $\hat{g}$ at all R by solving a 1-D Schrödinger equation

$$\left(-\frac{\hbar^2}{2\mu}\frac{d^2}{dR^2} + \frac{\hbar^2 \ell_i(\ell_i+1)}{2\mu R^2} + V^{lr} + \epsilon_{v_i j_i} - E\right)\begin{pmatrix}\hat{f}_i \\ \hat{g}_i\end{pmatrix} = 0 \tag{22}$$

subject to the boundary conditions (20) and (21). For H_2-H_2 scattering, beyond the strong interaction region, one only needs to deal with the weak, attractive van der Waals forces.

Hence, the MQDT reference functions can be obtained by choosing a long-range expansion for the reference potential, $V^{\rm lr} = -\frac{C_6}{R^6} - \frac{C_8}{R^8} - \frac{C_{10}}{R^{10}}$.

The matrix $\mathbf{K}^{\rm sr}$ and the linearly independent solutions, $\hat{f}$ and $\hat{g}$, carry all the information required to obtain the scattering observables. To obtain the physical scattering matrix, $\mathbf{S}^{\rm phys}$, four MQDT parameters $\mathcal{A}$, $\mathcal{G}$, η and γ are required in each channel [22]. These four quantities correctly describe the asymptotic behavior of the reference wave functions $\hat{f}$ and $\hat{g}$. Explicit expressions for these parameters are given in Eqs (12a) to (12d) in [22].

By partitioning $\mathbf{K}^{\rm sr}$ into energetically open (o) and closed (c) channels, we eliminate the unphysical growth inherent in $\mathbf{M}$ by the following transformation

$$\tilde{\mathbf{K}} = \mathbf{K}^{\rm sr}_{oo} - \mathbf{K}^{\rm sr}_{oc} \left(\cot\gamma + \mathbf{K}^{\rm sr}_{cc}\right)^{-1} \mathbf{K}^{\rm sr}_{co} \tag{23}$$

where $\cot\gamma$ is a diagonal matrix of dimension $N_c \times N_c$. Hence, $\tilde{\mathbf{K}}$, represents the N_o wave-functions with physical boundary conditions both at the origin and asymptotically. Roots of $\det(\mathbf{K}_{\rm cc} + \cot\gamma)$ approximate the locations of resonances in the cross section.

In order to relate $\tilde{\mathbf{K}}$ to $\mathbf{S}^{\rm phys}$, another set of energy-normalized, linearly independent solutions is required. For each energetically open channel, the reference functions f and g are defined as

$$f_i(R) \xrightarrow{R\to\infty} k_i^{-1/2} \sin(k_i R - \ell_i \pi/2 + \eta_i) \tag{24}$$

$$g_i(R) \xrightarrow{R\to\infty} -k_i^{-1/2} \cos(k_i R - \ell_i \pi/2 + \eta_i) \tag{25}$$

These functions are related to $\hat{f}$ and $\hat{g}$ through the following expressions,

$$f_i(R) = {\mathcal{A}_i}^{1/2} \hat{f}_i(R) \tag{26}$$

$$g_i(R) = {\mathcal{A}_i}^{-1/2} \mathcal{G}_i \hat{f}_i(R) + {\mathcal{A}_i}^{-1/2} \hat{g}_i(R). \tag{27}$$

Hence, $\mathbf{S}^{\rm phys}$ is obtained by the following series of simple transformations

$$\mathbf{K} = \mathcal{A}^{1/2} \tilde{\mathbf{K}} \left(I + \mathcal{G}\tilde{\mathbf{K}}\right)^{-1} \mathcal{A}^{1/2} \tag{28}$$

$$\mathbf{S}^{\rm phys} = e^{i\eta} \left(I + i\mathbf{K}\right) \left(I - i\mathbf{K}\right)^{-1} e^{i\eta} \tag{29}$$

where $\mathcal{A}$ and $\mathcal{G}$ and η are diagonal matrices of order $N_o \times N_o$ and I is the identity matrix.

III. RESULTS

Our main goal in this article is to demonstrate the power of the MQDT method for ultracold, non-resonant and quasi-resonant molecular scattering. To this end we wish to

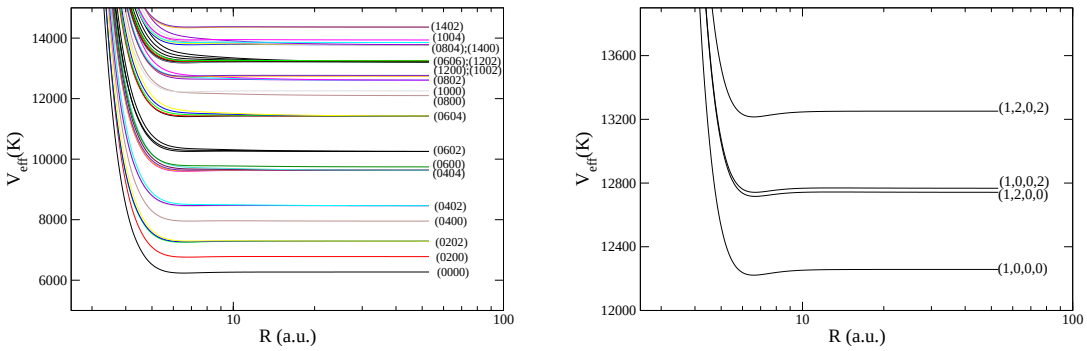

FIG. 1: Effective potential energy curves for para-H_2 scattering as defined in eq.(30). The labels for nearly degenerate curves are separated by a colon, where the highest lying threshold is on the right. The panel on the right shows the CMSs included in the basis set.

establish two criteria for H_2. First, that the separation between long and short-range physics is reasonable; and second, that the energy-dependent scattering may be easily described via an essentially energy-independent short-range wave function. We will also examine the sensitivity of results to the choice of the reference potential. To address these criteria, we will focus on H_2 collisions in which energy is nontrivially transferred among vibrational and rotational degrees of freedom between the two molecules.

A. Quasi-resonant scattering: convergence with respect to matching distance R_m

To establish the use of MQDT as a reasonable separation between short- and long-range behavior, we choose a problem where nontrivial energy exchange occurs in the short-range physics. The specific example is one of "quasi-resonant" energy transfer in para-para H_2 scattering, whereby two units of rotational angular momentum are transferred from a vibrationless molecule to a vibrating molecule [32, 34]. To illustrate this process, diabatic potential energy curves for two interacting para-H_2 molecules versus the intermolecular separation R are shown in Fig. 1. These are effective potentials, defined as

$$V_{eff}(R) = \epsilon_{vj} + \mathcal{U}^{JM\epsilon_I\epsilon_P}_{vj\ell,vj\ell}(R) + \frac{\hbar^2\ell(\ell+1)}{2\mu R^2}. \tag{30}$$

The particular quasi-resonant process of interest takes the initial channel $(v_1, j_1, v_2, j_2) = (1, 0, 0, 2)$ to $(1, 2, 0, 0)$. The name quasi-resonant pertains to the fact that the thresholds of

these channels are nearly degenerate, as seen in Fig. 1. Specifically, their energy separation, 25.45 K, is comparable to the well depth of the isotropic part of the H_2-H_2 interaction $\sim$ 31.7 K. The slightly different centrifugal distortion of the vibrational levels $v = 0$ and $v = 1$ is responsible for this small energy gap between the two CMSs. In this process the total rotational angular momentum is conserved by the collision. These kinds of transitions which have a small internal energy and internal rotational angular momentum gaps are found to be very efficient and highly state-selective and have been referred to as quasi-resonant rotation-rotation (QRRR) transfer [34]. Note that alternative final states are also possible, but the one we have selected is known to be the dominant one. Indeed, as illustrated in [35, 36], to accurately describe such quasi-resonant energy transfer, one does not need to couple any other $v,\ j$ levels in the basis set. One can restrict the basis set in the CC calculations to just those involved in the quasi-resonant transition yet still get results comparable to those from a larger basis set that includes many other CMSs. Thus, for the purpose of simplicity, we have resorted to a small basis (1,0,0,0),(1,0,0,2),(1,2,0,0) and (1,2,0,2) (as shown in the right panel of Fig. 1) that primarily includes the quasi-resonant channels in the CC calculations.

Using the restricted basis set described above, we have computed scattering cross sections for this process using the full CC calculation and the MQDT formalism. In the full CC calculation asymptotic matching to free-particle wave functions is carried out at R_∞= 100 a_0. In the MQDT approach, reference functions are determined from both the isotropic parts of the diagonal elements of the long-range diabatic potential coupling matrix, $\mathcal{U}^{JM\epsilon_I\epsilon_P}_{vj\ell,vj\ell}(R)$, and also the long-range approximation for the reference potential, $V^{\rm lr} = -\frac{C_6}{R^6} - \frac{C_8}{R^8} - \frac{C_{10}}{R^{10}}$. As discussed in the next subsection, we find that more accurate results are obtained when the long-range part of the diabatic potential curves are employed.

First, we establish convergence of elastic and inelastic cross sections as a function of the short-range matching distance R_m. Results of these studies are shown in Figure 2, for elastic (left panel) and inelastic QRRR (right panel) scattering. The QRRR transition is the dominant inelastic channel that corresponds to total angular momentum $J = 2$ and s-wave scattering in the incident channel. The solid black curve refers to results from the full close-coupling calculation, while the other curves correspond to the MQDT results for various values of the matching radius R_m. The convergence with respect to R_m is excellent and occurs as soon as R_m exceeds the region of the van der Waals well. The MQDT calculations are converged and nearly quantitatively reproduce the results from the full CC calculation

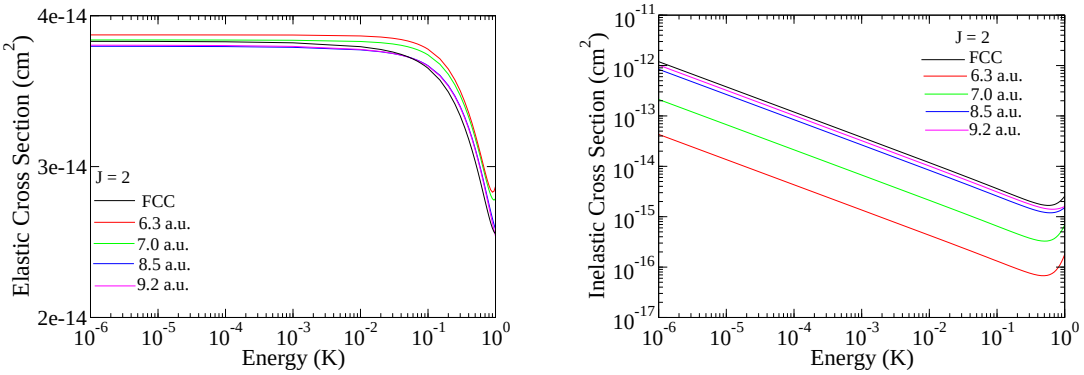

FIG. 2: Elastic (left) and inelastic (right) cross sections for (1,0,0,2) to (1,2,0,0) quasi-resonant scattering in para-H_2. The black curves correspond to the full CC calculation, while the other curves correspond to the MQDT result with different matching radii, R_m.

for a matching distance of R_m=9.2 $a.u.$ Note that the van der Waals length, $r_{\rm vdw} = \left(\frac{2\mu C_6}{\hbar^2}\right)^{1/4}$ for H_2-H_2 is 14.5 a_0. The agreement is also nearly quantitative for elastic scattering cross sections shown in the left panel. Although, for elastic scattering, the results are less sensitive to the matching distance. It should be emphasized that these convergence tests involve a single short-range $\mathbf{K}^{\rm sr}$ matrix computed at an initial collision energy of 1 μK, which is able to capture the dynamics at other collision energies in 1 μK-1 K range. This is an important aspect of MQDT calculations as discussed in more detail below.

B. Choice of reference potential and energy independent parameters

A key aspect of MQDT is to simplify the calculation and description of scattering, especially at ultracold temperatures. We have already demonstrated this for the para-para case where an energy independent short range $\mathbf{K}^{\rm sr}$ is able to reproduce cross sections over a wide range of energies when resonances are absent. An equally important issue is the choice of reference potential for the evaluation of MQDT reference functions. While for atom-atom scattering the obvious choice is the long-range expansion, for complex systems such as the present case, a more accurate choice given by the effective potential of Eq.(30) may be adopted. To explore these issues we consider similar quasi-resonant energy transfer in ortho-ortho and ortho-para collisions. Further, we extend the energy range of these calculations to 10 K to capture a d-wave shape resonance reported in an earlier work [35].

Similar to the case of para-H_2, here we consider a QRRR process in which an ortho-$H_2(v = 1, j = 1)$ molecule hits another vibrationless ortho-$H_2(v = 0, j = 3)$ molecule and takes away two units of rotational angular momentum. The process is described as $(v_1, j_1, v_2, j_2) = (1, 1, 0, 3) \rightarrow (1, 3, 0, 1)$. In this case the energy difference between the two threshold channels is 45.5 K. Full CC calculations have been reported for this process previously [35, 36], but we show results for the positive exchange symmetry to compare with MQDT in Fig.3. The elastic cross section is calculated according to equation (16). Only cross-sections for total angular momentum $J = 2$ that include s-wave scattering in the incident channel are shown. The solid black curve denotes the full CC result for both elastic (left panel) and inelastic (right panel) collisions obtained by matching to free particle wave functions at R_∞= $100a_0$.

MQDT results are obtained using a short-range matching distance of 9.5 a_0. The different curves for MQDT refer to different choices for the reference potential. The red curve corresponds to using a simplified potential $V^{\rm lr} = -C_6/R^6$, while the green curve corresponds to the diagonal elements of the isotropic part of diabatic coupling matrix discussed above. Both results correspond to a single $\mathbf{K}^{\rm sr}$ matrix evaluated at 1 μK for the entire energy regime. Both reference potentials are able to identify the d-wave resonance near 1 K, but do not find its energy position particularly accurately. In addition, the very simplest reference potential struggles to reproduce the non-resonant elastic cross section near threshold since this potential does not deliver an accurate phase shift in the region $R_m < R < R_\infty$. The blue curves in Figure 3 are also obtained using the diabatic potential coupling matrix for the reference potential, but here $\mathbf{K}^{\rm sr}$ matrix has been evaluated at various energy values in the 1μK-10 K range followed by interpolation in a fine energy grid. This grid consists of three different regions: (i) in the ultralow energy range, E_c = 1μK - 100 mK, $\mathbf{K}^{\rm sr}$ matrix is evaluated at 1μK, 1 mK and 100 mK; (ii) at low energies in the range E_c=200 mK-1 K, $\mathbf{K}^{\rm sr}$ is evaluated at 9 points with 100 mK separation; (iii) from 1 K - 10 K, an energy spacing of 1 K was employed. In this case the MQDT reproduces the full CC result quite well. MQDT identifies the resonance position and lineshape and matches the background cross sections at the percent level.

The ability to interpolate the short-range K-matrix and still get quantitative results stems from the smoothness of this quantity in energy, as shown in Fig. 4. Only elements corresponding to the quasi-resonant channels (1,1,0,3 and 1,3,0,1) are shown. Although the

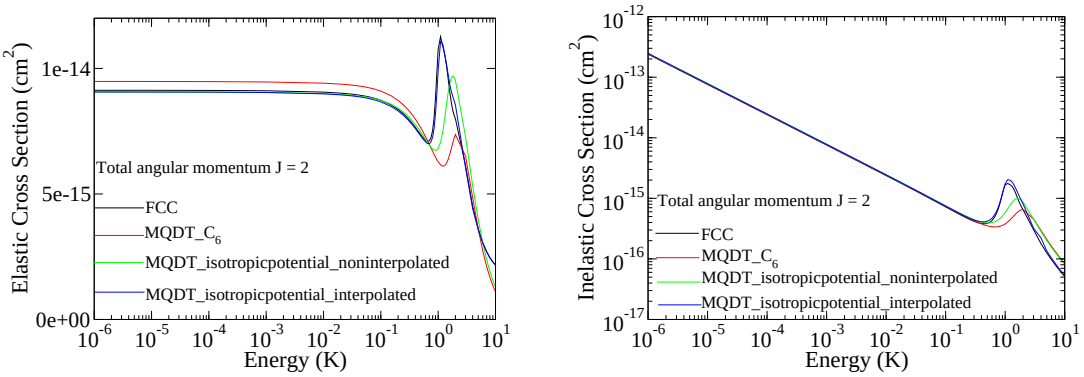

FIG. 3: This figure shows the elastic cross section for $H_2(v=1,j=1)$+$H_2(v=0,j=3)$ collisions (left panel) and the inelastic cross section for $H_2(v=1,j=1)$+$H_2(v=0,j=3) \rightarrow H_2(v=1,j=3)$+$H_2(v=0,j=1)$ quasi-resonant process (right panel).

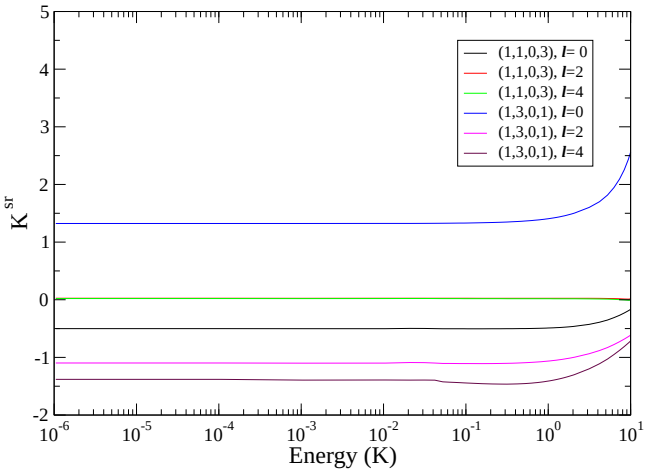

FIG. 4: Diagonal elements of the short-range K-matrix corresponding to the quasi-resonant transition [(1,3,0,1) $\rightarrow$ (1,1,0,3)] as a function of the collision energy. The isotropic part of the diabatic potential matrix elements is used for the reference potential and the matching radius $R_m = 9.5\ a_0$.

partial waves, $\ell = 2$ and 4 are present in both the initial and final channels, the dominant contribution comes from $\ell = 0$ for $E_c = 1\mu$K$-$ 1 K. It is clear from Fig.4 that up to 1 K the short-range K-matrix is independent of energy, but it becomes a smooth function of energy beyond 1 K. Thus, an energy independent short-range K-matrix evaluated at 1μK cannot be expected to adequately reproduce a shape resonance near 1 K.

Also, we note that the well depth of the isotropic part of the diabatic potential is only $\sim$ 31.7 K. When the collision energy becomes a significant fraction of the potential well depth the $\mathbf{K}^{\rm sr}$ matrix becomes a strong function of energy, and its energy dependence needs to be taken into account. Thus, for systems such as H_2+H_2 characterized by a relatively shallow van der Waals well, the energy dependence of the short-range K-matrix becomes important in describing the resonances supported by the van der Waals well. For other systems with deeper potential wells, one may be able to use an energy independent $\mathbf{K}^{\rm sr}$ matrix over a wider range of scattering energies. It is also possible that the MQDT treatment will need modification to handle resonances already present in $\mathbf{K}^{\rm sr}$ [16].

Next, we demonstrate the ability of the MQDT method to describe physics driven by vibrational, rather than rotational, dynamics. Specifically, we consider a second type of H_2 scattering, wherein a vibrationless ortho-H_2 hits a para-H_2 molecule that carries one quantum of vibration, transferring this vibration to the ortho molecule [36]. In our notation, para-$H_2(v=1,j=0)$+ortho-$H_2(v=0,j=1) \rightarrow$ para-$H_2(v=0,j=0)$ +ortho-$H_2(v=1,j=1)$ i.e, $(1,0,0,1) \rightarrow (0,0,1,1)$. Despite a small energy gap (8.5 K) between the initial and final states, one observes a surprisingly small inelastic cross section. This is because, due to the homonuclear symmetry of the H_2 molecules, the transfer of rotational energy between $j=0$ and $j=1$ states is symmetry forbidden. Hence the entire process is driven by vibrational energy transfer, which is generally less efficient than rotational energy transfer [34].

The resulting cross sections, computed according to the same three degrees of approximation as in Figure 3, are presented in Fig. 5, along with that from full CC calculations. The left panel depicts the elastic cross sections, and the right panel shows the inelastic counterparts. These cross sections were computed for total angular momentum $J=1$ to account for the dominant s-wave scattering in the incident channel at ultralow energies. A matching radius of $R_m = 9.5\ a_0$ is used for the MQDT calculations.

The solid black curve in Fig. 5 denotes the full close-coupling results computed on an energy grid of 10μK. The blue curve corresponds to MQDT calculations in which an interpolation scheme similar to that of the ortho-ortho case is adopted for the short range $\mathbf{K}^{\rm sr}$ matrix. The green curve represents the same calculation, assuming $\mathbf{K}^{\rm sr}$ (computed at $E_c = 1\mu$K) is valid at all energies. Like the ortho-ortho case both the blue (interpolated) and green (non-interpolated) curves almost exactly follow the black curve in the Wigner-threshold region, but the green curve begins to deviate above 100 mK as the resonance

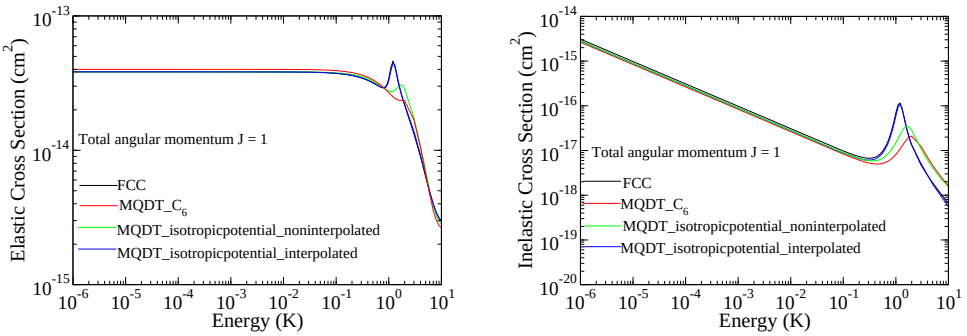

FIG. 5: Elastic (left) and inelastic (right) cross sections for ortho-para scattering of H_2. The black curves represent the full CC calculation, while the other curves denote different MQDT results as described in the text below.

region is approached.

It is abundantly clear from the above discussion that while a single $\mathbf{K}^{\rm sr}$ matrix is not capable of reproducing the dynamics over the entire energy range, including the resonance region, it is able to accurately describe the dynamics in the Wigner threshold regime. The accuracy of both the elastic and inelastic cross sections in the three cases considered validates the key idea of MQDT: the energy dependence of scattering observables is entirely tractable within the simple behavior of the long-range physics. We also emphasize that the method remains numerically tractable all the way down to 1μ K, about seven orders of magnitude lower in energy than the height of the centrifugal barriers. At 1μ K (and throughout the Wigner threshold regime) the elastic cross sections from the MQDT and full CC calculations agree to within 0.2–4% for all three initial states considered here. The corresponding inelastic cross sections agree to witin 3–10%. Finally, we note that the MQDT calculations are also accurate for partial waves $\ell = 1$, and 2 arising from other values of J (e.g., $J = 0$, 1 for ortho-ortho and $J = 0$, 2 for ortho-para) although they do not contribute significantly to the cross sections and hence not shown.

IV. CONCLUSIONS

We have presented a hybrid approach that combines full close-coupling calculations at short-range with the MQDT formalism at long-range to evaluate cross sections for elastic and quasi-resonant inelastic scattering in collisions of H_2 molecules. It is found that the full

CC calculation can be restricted to a relatively short-range, $\sim 9.0\ a.u$, which is just outside the region of the van der Waals potential well. Beyond this region, the scattering process is described within the MQDT formalism. Further, it is found that one may use a single short-range K-matrix, computed at say 1μK, to evaluate cross sections at energies all the way into the mK range, leading to significant savings in computational time. This works as long as scattering resonances are absent. When resonances are present, the short-range K-matrix becomes sensitive to energy and an interpolation of its elements computed on a relatively sparse grid in energy may be employed to yield reliable results.

The choice of H_2-H_2 for the present work is in part motivated by the possibility of full-dimensional CC calculations with no approximations (other than basis set truncation). However, due to its shallow van der Waals potential well, it is probably not the system for which MQDT provides the most accurate values. This is because, at the short range matching distance, for collision energies in the Kelvin range, the interaction potential becomes comparable to the scattering energy and determination of an energy independent short-range K-matrix is no longer possible. Furthermore, extending the calculations to energies beyond 1 K becomes difficult as the effective potential for $\ell > 2$ becomes positive for all values of R and computation of MQDT reference functions becomes difficult. Nevertheless, the hybrid approach seems to be very promising, and the savings in computations will be more dramatic when considering open shell systems with spin, hyperfine levels, and magnetic field effects.

While the results demonstrate the relevance of the MQDT approach in ultracold molecule-molecule scattering, there is still much to be developed. The treatment of resonances has become mundane in atom-atom scattering, but remains to be adequately developed for cold molecules [16]. Also, the long-range PES for H_2-H_2 remains reasonably isotropic, so that complete isotropy could be assumed when constructing the reference functions. Potentials with stronger anisotropies may necessitate a different long-range treatment, owing to strong interchannel couplings. Finally, for truly reactive systems, such as F+H_2, the short-range calculation is more conveniently carried out in hyperspherical, rather than Jacobi coordinates, in which case the application of MQDT needs to be modified to accommodate the transition between short- and long-range coordinate systems, as well as between short- and long-range wave functions. Such calculations are in progress.

V. ACKNOWLEDGEMENTS

This work was supported in part by NSF grant PHY-1205838 (N.B.) and ARO MURI grant No. W911NF-12-1-0476 (N.B. and J.L.B). Computational support by National Supercomputing Center for Energy and the Environment at UNLV is gratefully acknowledged. JH is grateful to Brian Kendrick for many helpful discussions.

---

[1] S. Ospelkaus, K.-K. Ni, G. Quéméner, B. Neyenhuis, D. Wang, M. H. G. de Miranda, J. L. Bohn, J. Ye, and D. S. Jin, Phys. Rev. Lett. **104**, 030402 (2010).

[2] For example, R. V. Krems, W. C. Stwalley, B. Friedrich, Eds., *Cold Molecules: Theory, Experiment, Applications* (Boca Raton, CRC Press, 2009).

[3] M. J. Seaton, Proc. Phys. Soc. London **88**, 801 (1966).

[4] M. J. Seaton, Rep. Prog. Phys. **46**, 167 (1983).

[5] U. Fano and A. R. P. Rau, Atomic Collisions and Spectra (Academic Press, Orlando, FL, 1986).

[6] F. H. Mies, J. Chem. Phys. **80**, 2514 (1984).

[7] C. H. Greene, A. R. P. Rau, and U. Fano, Phys. Rev. A **30**, 3321 (1984).

[8] J. P. Burke, C. H. Greene, and J. L. Bohn, Phys. Rev. Lett. **81**, 3355 (1998).

[9] F. H. Mies and M. Raoult, Phys. Rev. A **62**, 012708 (2000).

[10] M. Raoult and F. H. Mies, Phys. Rev. A **70**, 012710 (2004).

[11] B. Gao, E. Tiesinga, C. J. Williams, and P. S. Julienne, Phys. Rev. A **72**, 042719 (2005).

[12] T. M. Hanna, E. Tiesinga, and P. S. Julienne, Phys. Rev. A **79**, 040701 (2009).

[13] Z. Idziaszek, T. Calarco, P. S. Julienne, and A. Simoni, Phys. Rev. A **79**, 010702 (2009).

[14] B. Gao, Phys. Rev. Lett. **104**, 213201 (2010).

[15] J. F. E. Croft, A. O. G. Wallis, J. M. Hutson, and P. S. Julienne, Phys. Rev. A **84**, 042703 (2011).

[16] J. F. E. Croft, J. M. Hutson, and P. S. Julienne, Phys. Rev. A **86**, 022711 (2012).

[17] Z. Idziaszek and P. S. Julienne, Phys. Rev. Lett. **104**, 113202 (2010).

[18] Z. Idziaszek, G. Quéméner, J. L. Bohn, and P. S. Julienne, Phys. Rev. A 82, 020703 (2010).

[19] B. Gao, Phys. Rev. Lett. **105**, 263203 (2010).

[20] G. R. Wang, T. Xie, Y. Huang, W. Zhang, and S.L. Cong, Phys. Rev. A **86**, 062704 (2012).

[21] R. Pires, M. Repp, J. Ulmanis, E. D. Kuhnle, M. Weidemüller, T. G. Tiecke, C. H. Greene, B. P. Ruzic, J. L. Bohn, and E. Tiemann, Phys. Rev. A (accepted, 2014).

[22] B. P. Ruzic, C. H. Greene, and J. L. Bohn, Phys. Rev. A **87**, 032706 (2013).

[23] K. Takayanagi, Adv. At. Mol. Phys. **1**, 149 (1965).

[24] S. Green, J. Chem. Phys. **62**, 2271 (1975).

[25] M. H. Alexander and A. E. DePristo, J. Chem. Phys. **66**, 2166 (1977).

[26] S. K. Pogrebnya and D. C. Clary, Chem. Phys. Lett. **363**, 523 (2002).

[27] G. Quéméner and N. Balakrishnan, J. Chem. Phys. **130**, 114303 (2009).

[28] A. M. Arthurs and A. Dalgarno, Proc. R. Soc. London, Ser. A **256**, 540 (1960).

[29] B. R. Johnson, J. Comput. Phys. **13**, 445 (1973).

[30] D. E. Manolopoulos, J. Chem. Phys. **85**, 6425 (1986).

[31] M. Abramowitz and I. S. Stegun, Handbook of Mathematical Functions, U.S. Govern- ment Printing Office, Washington, DC, (1964).

[32] N. Balakrishnan, G. Quéméner, R.C. Forrey, R. J. Hinde and P. C. Stancil, J. Chem. Phys. **134**, 014301 (2011).

[33] C. H. Greene, A. R. P. Rau, and U. Fano, Phys. Rev. A **30**, 3321 (1984).

[34] G. Quéméner, N. Balakrishnan, and R. V. Krems, Phys. Rev. A **77**, 030704(R) (2008).

[35] S. Fonseca dos Santos, N. Balakrishnan, S. Lepp, Quéméner, R. C. Forrey, R. J. Hinde, and P. C. Stancil, J. Chem. Phys. **134**, 214303 (2011).

[36] S. Fonseca dos Santos, N. Balakrishnan, R. C. Forrey, and P. C. Stancil, J. Chem. Phys. **138**, 104302 (2013).

[37] B. Gao, Phys. Rev. A **58** 1728 (1998).